Journal of Machine Engineering, 2019, Vol. 19, No. 2, 32–45
ISSN 1895-7595 (Print) ISSN 2391-8071 (Online)

Received: *21 December 2018* / Accepted: *16 April 2019* / Published online: *29 June 2019*

modal control, active vibration control,
machine tool, inertial actuator

Christoph PEUKERT[1*]
Patrick PÖHLMANN[1]
Marcel MERX[1]
Jens MÜLLER[1]
Steffen IHLENFELDT[1,2]

INVESTIGATION OF LOCAL AND MODAL BASED ACTIVE VIBRATION CONTROL STRATEGIES ON THE EXAMPLE OF AN ELASTIC SYSTEM

Nowadays, feed axes are often equipped with multiple parallel-acting actuators in order to increase the dynamics of the machine tool. Also, additional actuators for active damping are widely used. Normally, the drives or actuators are controlled independently without consideration for the impact on each other. In contrast, by using the modal space control, the system can be decoupled and the modal control loops can be adjusted independently. This control approach is particularly suitable for motion systems, such as machine tools, which have more drives or actuators than degrees of freedom of movement. This paper deals with the pre-investigation of the modal-based vibration control for machine tools with additional actuators. The object of investigation is an elastic system with a movable saddle. The modal-based control is compared with a local control approach. The results obtained experimentally on the test rig are presented. The modal control is superior since, with the modal approach, each control loop corresponds to a specific vibration mode, and the control law for this loop is designed to provide the desired performance of the control system at the corresponding resonance frequency. The parameterisation of the control loops is simplified by modal control, since the modes can be controlled independently.

1. INTRODUCTION

The primary focus in machine tool design is to increase the productivity of the machine tool whilst improving or maintaining their accuracy of motion. Additionally, a high energy efficiency of machine tools is aimed for. Amongst other methods, an increase of productivity is achievable by increasing the feed dynamics of the machines. This can be achieved by reducing the mass of the moving components or by increasing the driving forces. One way of increasing the drive forces is to use multiple parallel-acting actuators. Because of the mechanical coupling of the drives, undesirable interference of the actuators occurs.

[1] Technische Universität Dresden, Faculty of Mechanical Science and Engineering, Institute of Mechatronic Engineering, Chair of Machine Tools Development and Adaptive Controls, Dresden, Germany
[2] Fraunhofer Institute for Machine Tools and Forming Technology IWU, Dresden, Germany
[*] E-mail: christoph.peukert@tu-dresden.de
https://doi.org/10.5604/01.3001.0013.2222

By using compliant mechanisms to mechanically decouple the parallel-acting drives and the guide elements, the control bandwidth could be significantly increased and therefore the reference and disturbance behaviour are greatly improved [1]. However, an increase in motion dynamics (higher inertial forces) leads to a stronger vibrational excitation of machine structures. Therefore, measures to reduce the machine frame excitation were developed and investigated [2, 3]. In addition, there are measures to reduce the susceptibility of moving machine components to vibrations. This includes the structural lightweight design of the components (topology optimisation) [4], the material lightweight design (usage of carbon-fibre composites) [5] and the system lightweight design (adaptronics) [6]. Typically, the target criteria are defined as the maximisation of static and dynamic stiffness of the structure while minimising its mass. However, the moving masses cannot be reduced arbitrarily without a loss of stiffness. In order to estimate the minimum value for dynamic stiffness of the structural components, stability lobe diagrams are suitable [7, 8].

The dynamic stiffness of the machine components can be increased using dynamic auxiliary systems without having to intervene constructively in the machine tool structure. Brecher et al. characterise different concepts of auxiliary systems for passive and active damping of mechanic structures [9]. With the use of *Active Damping Devices* (ADDs) a higher power density can be achieved compared to passive systems. In [10] and [11] the application of ADDs on milling machines was investigated. It was shown that productivity and surface quality can be significantly increased.

Moreover, active systems which are integrated in the mechanical structure are developed to optimise its dynamic behaviour. In [12] piezoelectric actuators are used to increase the dynamic stiffness of a grinding machine. This is achieved by feeding the acceleration signals back. Denkena and Gümmer conducted comparable investigations on a milling machine [13]. Piezo actuators are integrated in the spindle system, which allows the modulation of the tool engagement by a dynamic signal. Kras et al. described a semi-active damping system, which is integrated in the tailstock of a lathe machine [14]. In order to reach both high stiffness and damping characteristics, viscoelastic ceramics are used. With the integration of piezo actuators, the parameters of the system can be adjusted.

Whether an auxiliary system is used or not, the design of the control-strategy plays an important role in the control of vibration. In [15], a method to preshape the command-input so that structural vibrations can be avoided is presented. Since it is a feedforward-scheme, there is no need for additional actuators. This method has been proven e.g. in the control of flexible manipulators like in [16] or [17].

In general, tuning of multi-variable systems, like machine tools, is not a straight-forward task, especially when parallel acting drives and additional actuators are used. In this context, modal control represents a promising concept since the control is easier to design and the input energy can be reduced [18]. In addition, independent modal-space control is insensitive to the locations of the actuators. The concept of independent modal control was introduced by Balas [19] and Meirovitch et al. [18] to handle flexible mechanical systems. This method is based on the modal decomposition of linear systems, and facilitates to control each vibration mode independently. The number of sensors and actuators used is decisive for the implementation of this control structure. The modal control strategy is applied in smart structures since the availability of numerous sensors and actuators is guaranteed [21]. In order

to reduce the number of required sensors, band-pass filters [22] or state observers [23] are used. Lindberg and Longman dealt with the problem of actuator placement on structures [24] and examined the usage of a low number of actuators. Baz and Poh developed an algorithm which allows for switching between the different modes that should be controlled [25]. On the basis of laboratory experiments, e.g. on beams or large flexible parts of spacecrafts, the effectiveness of modal control has been demonstrated in many experiments [21–23]. In [26] the local and modal control approach for vibration control of a beam are compared. The investigated types of control systems differ in the algorithm of the controller only. Frequency response design method is applied to obtain the transfer functions of the controllers. It was shown that the modal control system can suppress vibrations with high efficiency at both considered resonances.

Resta [27] used a modal state feedback in combination with a modal state-observer for the control of a flexible hydraulic manipulator. With this control-scheme, structural vibrations and therefore material stress can be reduced. In [28] a planar manipulator is examined. In order to raise the structural damping of the flexible elements, Zhang placed piezo-actuators and -sensors on their surface and used a modal control structure.

This article presents a preliminary study on the application of modal control for machine tools. In the example of an elastic system equipped with two inertial actuators, the modal control (MC) is investigated in order to suppress forced vibrations, and compared with a local control (LC) approach. While the MC is based on the modal transformations described in Section 2.1, the actuator-sensor pairs considered in the LC, form independent control loops. This means that the LC only feeds back local state information (acceleration) to each actuator [29]. In contrast to LC, with the MC, all signals are fed back into each modal controller.

In the 2nd section, the idea of the modal control, and an overview of resonant control strategies are presented. The object of investigation and the corresponding simulation model is briefly described in Section 3. Findings from experiments are demonstrated in Section 4.

2. MODAL CONTROL

2.1. MODAL DECOUPLING

The equation of motion of a discrete N-degree-of-freedom (DoF) mechanical system is given by

$$\boldsymbol{M}\ddot{\boldsymbol{q}} + \boldsymbol{D}\dot{\boldsymbol{q}} + \boldsymbol{K}\boldsymbol{q} = \boldsymbol{f}, \tag{1}$$

where $\boldsymbol{M}$, $\boldsymbol{D}$ and $\boldsymbol{K}$ are the matrices of inertia, damping and stiffness, $\boldsymbol{q}$ is the vector of the physical coordinates and $\boldsymbol{f}$ is the vector of the corresponding physical forces or torques. This equation can also be used as a discretised description of distributed-parameter systems, e.g. when finite element methods are used. With the matrix of the eigenvectors

$$\boldsymbol{\Phi} = (\boldsymbol{\varphi}_1 \quad \cdots \quad \boldsymbol{\varphi}_N), \tag{2}$$

which is the solution of the eigenvalue problem of the undamped system

$$(\boldsymbol{K} - \omega_i^2 \boldsymbol{M})\boldsymbol{\varphi}_i = 0, \tag{3}$$

the transformation between the modal $\boldsymbol{\xi}$ and the physical coordinates $\boldsymbol{q}$ can be achieved by:

$$\boldsymbol{q} = \boldsymbol{\Phi}\boldsymbol{\xi}. \tag{4}$$

The substitution of Eq. (4) into Eq. (1) and the left-multiplication by $\boldsymbol{\Phi}^{\mathrm{T}}$ gives the modal form of Eq. (1):

$$\ddot{\boldsymbol{\xi}} + \boldsymbol{\Delta}\dot{\boldsymbol{\xi}} + \boldsymbol{\Lambda}\boldsymbol{\xi} = \boldsymbol{\mu}^{-1}\boldsymbol{\tau}, \tag{5}$$

where $\boldsymbol{\tau} = \boldsymbol{\Phi}^{\mathrm{T}}\boldsymbol{f}$ is the vector of the modal forces, $\boldsymbol{\mu} = \mathrm{diag}(\mu_i)$ is the matrix of the modal masses and $\boldsymbol{\Lambda} = \mathrm{diag}(\omega_i^2)$ is the matrix of the eigenvalues. Since $\boldsymbol{\Phi}$ is the solution of the undamped problem in Eq. (3), $\boldsymbol{\Phi}^{\mathrm{T}}\boldsymbol{D}\boldsymbol{\Phi}$ has no diagonal form in general. With the condition of a slightly damped system, the matrix of the modal damping ratios $\boldsymbol{\Delta}$ is approximately defined by (see [30]):

$$\boldsymbol{\Delta} := \mathrm{diag}(2\delta_i). \tag{6}$$

According to these assumptions, the system given in Eq. (5) can be written as N independent second-order equations:

$$\ddot{\xi}_i + 2\delta_i\dot{\xi}_i + \omega_i^2\xi_i = \mu_i^{-1}\tau_i, \text{with } i = 1 \dots N. \tag{7}$$

The idea of the independent modal control is to control the modal systems in Eq. (7) directly, which can be seen as independent mass-spring-damper-systems. The modal control-laws are defined by:

$$\tau_{\mathrm{C},i} = R_i\left(\xi_{\mathrm{C},i}\right), \tag{8}$$

where each modal force $\tau_{\mathrm{C},i}$ depends on the actual amplitude of the corresponding vibration mode only. The whole control law is given by:

$$\boldsymbol{f}_{\mathrm{A}} = \boldsymbol{\Theta}\boldsymbol{\tau}_{\mathrm{C}} = \boldsymbol{\Theta}\boldsymbol{R}_{\mathrm{mod}}(\boldsymbol{\xi}_{\mathrm{C}}) \text{ and } \boldsymbol{\xi}_{\mathrm{C}} = \boldsymbol{\Psi}^{\mathbf{T}}\boldsymbol{q}_{\mathrm{S}}. \tag{9}$$

Since the system in Eq. (1) is a complex mechanical structure, not every physical coordinate can be measured. Therefore, $\boldsymbol{q}_{\mathrm{S}}$ is the vector of given measurements, which is part of the full vector $\boldsymbol{q}$. The vector of the actuator forces $\boldsymbol{f}_{\mathrm{A}}$ is selected from $\boldsymbol{f}$. $\boldsymbol{R}_{\mathrm{mod}}(\boldsymbol{\xi}_{\mathrm{C}})$ includes the modal control laws given in Eq. (8). In general, only a small number n_{C} of all modal subsystems with the modal coordinates $\boldsymbol{\xi}_{\mathrm{C}}$ is taken into account. The transformation between physical and estimated modal coordinates is done by the *modal filter* $\boldsymbol{\Psi}^{\mathbf{T}}$ [31]. In order to calculate the required actuator forces from the desired modal forces, the matrix $\boldsymbol{\Theta}$, also known as *modal synthesizer* [28], is used. These matrices can be calculated by:

$$\boldsymbol{\Psi}^{\mathbf{T}} = (\boldsymbol{\Phi}_{\mathrm{CS}})^{-1} \text{ and } \boldsymbol{\Theta} = (\boldsymbol{\Phi}_{\mathrm{CA}}^{\mathrm{T}})^{-1}, \tag{10}$$

where $\boldsymbol{\Phi}_{\mathrm{CS}}$ is a submatrix of $\boldsymbol{\Phi}$ containing only the columns of the controlled modes and the rows of the measurements, whereas for $\boldsymbol{\Phi}_{\mathrm{CA}}$ the rows of $\boldsymbol{\Phi}$ respecting the actuator placements are picked out. In case of collocated actuators and sensors, $\boldsymbol{\Phi}_{\mathrm{CS}}$ is equal to $\boldsymbol{\Phi}_{\mathrm{CA}}$ and can be thus referred to as $\boldsymbol{\Phi}_{\mathrm{C}}$. Since only a restricted number of actuators and sensors is used, the transformations between physical and modal space are incomplete. On the one hand, uncontrolled modal amplitudes also appear in the estimations of the controlled ones. On the other hand, the actuator forces can also excite the uncontrolled modes. These unwanted effects are called observation- and control-spillover (coupling between truncated and unmodelled

modes) and are explained in detail in [20, 32]. Furthermore, it is necessary to use as many sensors and actuators as controlled modes to calculate the inverse, indicated by Eq. (10).

A common method is the use of a modal state feedback

$$R_i\left(\xi_{\mathrm{C},i}\right) := k_{\mathrm{P},i}\xi_{\mathrm{C},i} + k_{\mathrm{V},i}\dot{\xi}_{\mathrm{C},i}, \tag{11}$$

to define the modal control laws (e.g. in [18, 19, 27, 32]). However, the aim of this work is to increase the damping of the system and to reduce vibrations caused by external disturbances. This can be achieved by using only velocity feedback and setting $k_{\mathrm{P},i}$ to zero. In this case, Eq. (7), (8) and (11) lead to:

$$\ddot{\xi}_{\mathrm{C},i} + 2\delta_i\dot{\xi}_{\mathrm{C},i} + \omega_i^2\xi_{\mathrm{C},i} = \mu_i^{-1}k_{\mathrm{V},i}\dot{\xi}_{\mathrm{C},i} \Longrightarrow \ddot{\xi}_{\mathrm{C},i} + \left(2\delta_i - \mu_i^{-1}k_{\mathrm{V},i}\right)\dot{\xi}_{\mathrm{C},i} + \omega_i^2\xi_{\mathrm{C},i} = 0, \tag{12}$$

which is also known as *Direct Velocity Feedback* (DVF) [34]. Nevertheless, in practice the measurement of velocity is elaborate. As shown later, the feedback of acceleration is more efficient, especially because sensors are cheap and no connection to the surrounding is necessary. A discussion of different control strategies follows in the next section.

2.2. RESONANT VIBRATION CONTROL

In terms of active vibration damping using a collocated actuator-sensor-configuration, the aim of the controller is to generate a force signal which has got a phase shift of 180° to the systems velocity [33, 34]. As mentioned before, this can be achieved by a direct feedback of a velocity signal. In a practical application, velocity-measurement is difficult. Another problem is that the correct phase shift cannot be guaranteed, especially for higher frequencies, since signal delays or a phase lag through actuators and sensors are present. However, there is a wide variety of transfer functions known as *Resonant Controllers* (RC) facing these problems (see [33]). One of the most commonly used strategies is the *Positive Position Feedback* (PPF) (e.g. [34, 35, 37]), whose transfer function is given by:

$$R(\mathrm{j}\omega) = \frac{k}{(\mathrm{j}\omega)^2 + 2\delta_{\mathrm{C}}(\mathrm{j}\omega) + \omega_{\mathrm{C}}^2}, \tag{13}$$

where δ_{C} and ω_{C} are parameters and k is the gain. The filter frequency ω_{C} is usually set to one of the systems eigenfrequencies, which should be damped. The complex-conjugated pole achieves a quick decrease of the transfer functions gain for higher or lower frequencies. Another example of a RC strategy is the *Negative Position Feedback* (NPF) presented in [37], which uses the same denominator term as PPF in Eq. (13) but a different numerator. The NPF can also be adapted for velocity or acceleration measurement by changing the numerator term of the transfer function. These functions are called *Negative Derivative Feedback* (NDF) [31] and *Negative Acceleration Feedback* (NAF). Table 1 gives an overview of the controller numerators.

Notice, that even if the numerators of NPF, NDF and NAF are different, the response of the controller with respect to the velocity of the system is the same. From this point of view, it is more advantageous to use NAF instead of NPF because of its low-pass character that allows for suppressing of the signal noise without the use of a separate filter.

Table 1. Measured signals and numerators of the transfer function of commonly used RC

	PPF	NPF	NDF	NAF
Measured signal	Position	Position	Velocity	Acceleration
Numerator	k	$-k(\mathrm{j}\omega)^2$	$-k(\mathrm{j}\omega)$	$-k$

3. STRUCTURE OF THE TEST RIG AND THE ASSOCIATED MODEL

The object of investigation is an elastic system with a movable saddle, which is clampable on the linear guiding rail. The test rig is equipped with two ADDs (ADD-45N, Micromega®) and two piezoelectric-accelerometers (see Fig. 1). The ADDs are active systems consisting of a control system based on sensors/actuators, as well as power electronics, and can easily be installed on an existing machine to improve its dynamic behaviour. In this paper, only the current controllers are used.

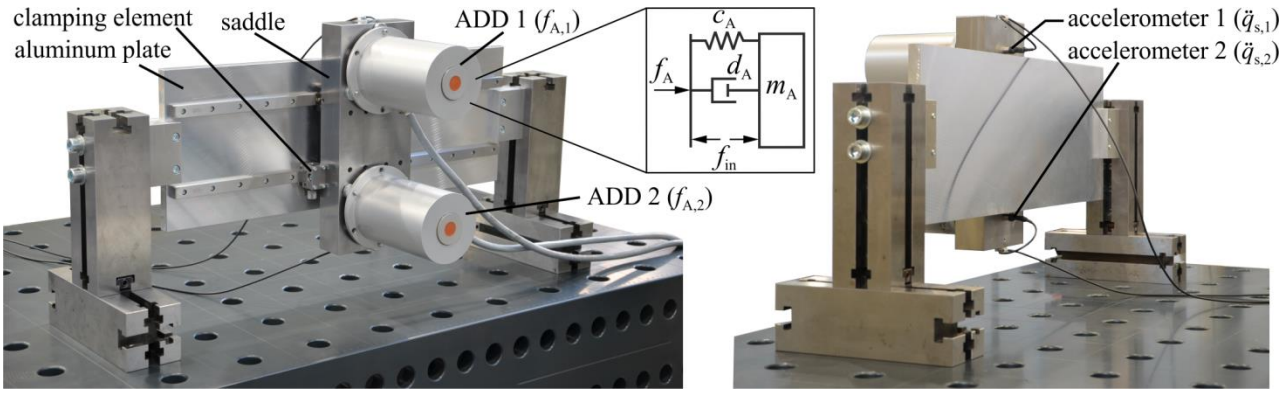

Fig. 1. Test rig with two ADDs and two accelerometers: front (left) and rear view (right)

The physical principle of the inertial actuator, also known as proof-mass actuator [34], is depicted in Fig. 1. The force f_{in}, which is generated by a voice coil, acts on the structure as well as on the free moveable mass m_{A}. The connection between the static and moving part of the actuator can be modelled as a spring-damper-element (c_{A}, d_{A}). The transfer function is given by:

$$\frac{f_{\mathrm{A}}}{f_{\mathrm{in}}} = \frac{m_{\mathrm{A}}(\mathrm{j}\omega)^2}{m_{\mathrm{A}}(\mathrm{j}\omega)^2 + d_{\mathrm{A}}(\mathrm{j}\omega) + c_{\mathrm{A}}} = \frac{(\mathrm{j}\omega)^2}{(\mathrm{j}\omega)^2 + 2\delta_{\mathrm{A}}(\mathrm{j}\omega) + \omega_{\mathrm{A}}^2}. \tag{14}$$

This dynamic behaviour can be ignored for high frequencies ($\omega \gg \omega_{\mathrm{A}}$) and therefore f_{A} is approximately equal to f_{in} [34]. The force of the voice coil f_{in} is proportional to the electric current i, which is controlled by an amplifier with an internal current control loop. The different feedback controllers for MC and LC are implemented in TwinCAT®. Several EtherCAT® terminals are used to enable the connection of the sensors/actuators. The communication between the sensors/actuators and the control unit is realised by an EtherCAT® fieldbus.

A numerical model was developed in order to conduct simulative investigations regarding suitable control concepts, optimal sensor/actuator placements and to estimate the parameters for different control strategies. The model was also used for the preliminary design of the components of the test rig. The mechanical components were modelled with ANSYS®. Since the ADDs, as part of the elastic system, significantly influence the dynamic behaviour of the test structure under consideration, they have to be taken into account in the model. By applying a modal order reduction technique, the dynamic characteristics of the components were included in an elastic multibody simulation carried out with MATLAB/Simulink®. After the test rig had been set up, experimental modal analyses of the individual components and assemblies were carried out to validate the model step by step. The comparison of the simulated and measured dynamic behaviour of the assembled test rig is depicted in Fig. 2. It is evident that the frequency response of the test rig is accurately reproduced up to approximately 350 Hz. Additionally, the location of excitation (f_{Imp}) and the corresponding acceleration measurement ($\ddot{q}_{\mathrm{Imp}}$), as well as the relevant mode shapes, are illustrated in Fig. 2. For the *Frequency Response Functions* (FRFs) shown in Fig. 2, the saddle was not clamped.

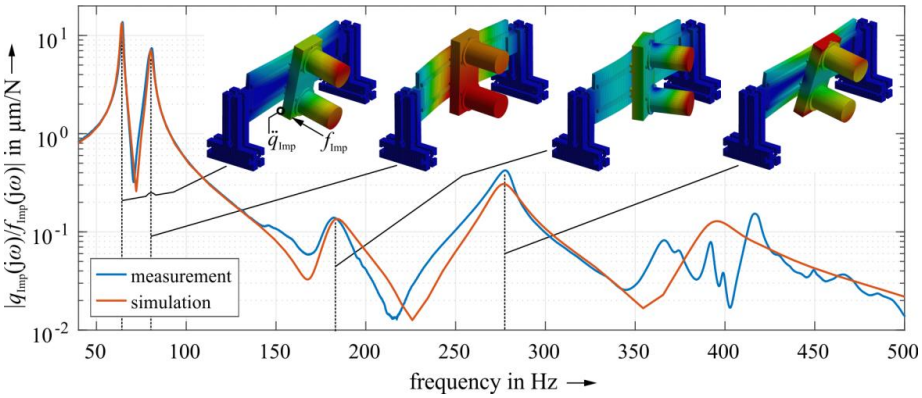

Fig. 2. Comparison of the measured and simulated FRF as well as the first four characteristic mode shapes

4. EXPERIMENTAL ANALYSIS OF THE CONTROL STRATEGIES

4.1. MODE SEPARATION

One important point of the experiments is the identification of the systems behaviour in the frequency domain. Since the system has two inputs and two outputs, four transfer functions can be measured:

$$\begin{pmatrix} q_{\mathrm{S},1} \\ q_{\mathrm{S},2} \end{pmatrix} = \underbrace{\begin{pmatrix} G_{11}(\mathrm{j}\omega) & G_{12}(\mathrm{j}\omega) \\ G_{21}(\mathrm{j}\omega) & G_{22}(\mathrm{j}\omega) \end{pmatrix}}_{\boldsymbol{G}(\mathrm{j}\omega)} \cdot \begin{pmatrix} f_{\mathrm{A},1} \\ f_{\mathrm{A},2} \end{pmatrix}. \tag{15}$$

In order to identify the system, a pseudo-random-sequence is used as command signal for both actuators. The advantage of this signal is that a wide frequency range can be excited.

With the measurement of the acceleration signals $\ddot{q}_{S,1}$ and $\ddot{q}_{S,2}$ the four transfer functions are obtained. The integration of the acceleration signals is conducted in the frequency domain. The FRFs $|G_{11}(\mathrm{j}\omega)|$ and $|G_{22}(\mathrm{j}\omega)|$ are illustrated in Fig. 3. With the knowledge of the entire system $\boldsymbol{G}(\mathrm{j}\omega)$ the modal parameters listed in Table 2 are calculated. The same method is used to identify the closed loop performance of the implemented controllers. Since only a two-variable control is considered in this paper (two inputs and two outputs), with the modal control, only two modes can be decoupled and independently controlled.

Table 2. Experimentally determinated modal parameters of the first two eigenmodes

Mode i	Frequency in Hz $\omega_{C,i}/(2\pi)$	Elements of the modal matrix $\boldsymbol{\Phi}_C^T$	
		$q_{S,1}/\xi_{C,i}$	$q_{S,2}/\xi_{C,i}$
1	65.1	0.763	−0.647
2	83.5	0.664	0.748

The entries of the measured modal matrix $\boldsymbol{\Phi}_C = (\boldsymbol{\varphi}_{C,1} \quad \boldsymbol{\varphi}_{C,2})$ are normalised so that the lengths of the eigenvectors $\boldsymbol{\varphi}_{C,1}$ and $\boldsymbol{\varphi}_{C,2}$ are equal to 1. With Eq. (10) the *modal filter* $\boldsymbol{\Psi}^T$ and the *modal synthesizer* $\boldsymbol{\Theta}$ can be defined in order to implement a modal control system:

$$\boldsymbol{\Psi}^T = \begin{pmatrix} 0.748 & -0.664 \\ 0.647 & 0.763 \end{pmatrix}, \quad \boldsymbol{\Theta} = \begin{pmatrix} 0.748 & 0.647 \\ -0.664 & 0.763 \end{pmatrix}. \tag{16}$$

To prove the decoupling effect, the modal transfer function matrix of the system $\boldsymbol{G}_{\mathrm{mod}}$ is calculated, where $\boldsymbol{\Psi}^T$ and $\boldsymbol{\Theta}$ are used to transform the inputs and outputs:

$$\begin{pmatrix} \xi_{C,1} \\ \xi_{C,2} \end{pmatrix} = \underbrace{\boldsymbol{\Psi}^T \cdot \boldsymbol{G}(\mathrm{j}\omega) \cdot \boldsymbol{\Theta}}_{\boldsymbol{G}_{\mathrm{mod}}(\mathrm{j}\omega)} \cdot \begin{pmatrix} \tau_{C,1} \\ \tau_{C,2} \end{pmatrix} = \begin{pmatrix} G_{\mathrm{mod},11}(\mathrm{j}\omega) & G_{\mathrm{mod},12}(\mathrm{j}\omega) \\ G_{\mathrm{mod},21}(\mathrm{j}\omega) & G_{\mathrm{mod},22}(\mathrm{j}\omega) \end{pmatrix} \cdot \begin{pmatrix} \tau_{C,1} \\ \tau_{C,2} \end{pmatrix}. \tag{17}$$

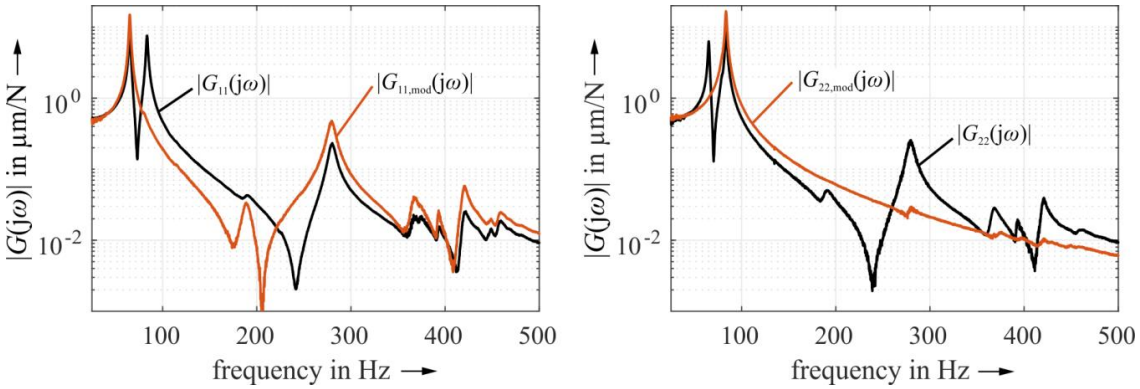

Fig. 3. Comparison of the measured open loop FRFs (excitation with ADD)

The FRFs $\left|G_{\mathrm{mod},11}(\mathrm{j}\omega)\right|$ and $\left|G_{\mathrm{mod},22}(\mathrm{j}\omega)\right|$ are shown in Fig. 3. The first two modes only appear in one of the FRFs, so the mode separation is performed correctly. The other peaks at higher frequencies do not disappear (spillover effect). Since the transformation in Eq. (16) considers the first two modes only, the other modes cannot be separated. An interesting point is that the peaks between 150 Hz and 500 Hz are mainly located in

$G_{\mathrm{mod},11}$ and not in $G_{\mathrm{mod},22}$, so their mode shape appears to be comparable to the shape $\boldsymbol{\varphi}_{\mathrm{C},1}$ of the first mode.

4.2. MODAL VIBRATION CONTROL

In this section, the MC is investigated and compared with the LC. Both control schemes are displayed Fig. 4.

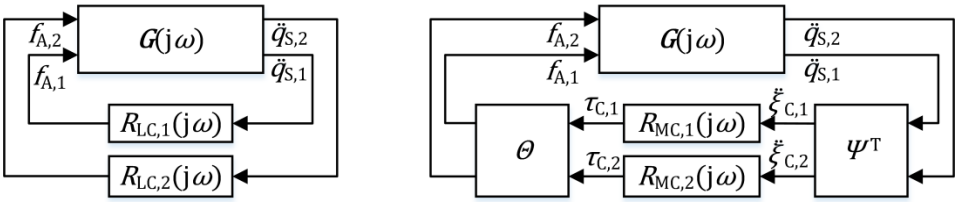

Fig. 4. Block diagram of the control logics: LC (left) and MC (right)

As previously noted, two NAF-transfer functions are used, where each of them is tuned to one of the eigenfrequencies given in Table 2. The four control laws of MC and LC are defined by:

$$R_{\mathrm{LC},1} = k_{\mathrm{LC},1}(NAF_1 + NAF_2) \text{ and } R_{\mathrm{LC},2} = k_{\mathrm{LC},2}(NAF_1 + NAF_2)\,, \tag{18}$$

$$R_{\mathrm{MC},1} = k_{\mathrm{MC},1} \cdot NAF_1 \text{ and } R_{\mathrm{MC},2} = k_{\mathrm{MC},2} \cdot NAF_2 \tag{19}$$

$$\text{where } NAF_1 := \frac{-2\delta_{\mathrm{C},1}}{(\mathrm{j}\omega)^2 + 2\delta_{\mathrm{C},1}(\mathrm{j}\omega) + \omega_{\mathrm{C},1}^2} \text{ and } NAF_2 := \frac{-2\delta_{\mathrm{C},2}}{(\mathrm{j}\omega)^2 + 2\delta_{\mathrm{C},2}(\mathrm{j}\omega) + \omega_{\mathrm{C},2}^2}. \tag{20}$$

The parameters $\delta_{\mathrm{C},i}$ are chosen to be $\delta_{\mathrm{C},i} := 0.4 \cdot \omega_{\mathrm{C},i}$ in each case. The unit of the gains $k_{\mathrm{LC,i}}$ and $k_{\mathrm{MC,i}}$ is Ns^2/m, but this is omitted in the remainder of the paper. Since both peaks of mode one and two appear in each coordinate $q_{\mathrm{S},1}$ and $q_{\mathrm{S},2}$ both of the NAF-functions are implemented in each controller of the local approach. For the MC, only one NAF-function in each loop is necessary. $\omega_{\mathrm{C},1}$ e.g. is the resonance frequency that appears in $G_{\mathrm{mod},11}$ (see Fig. 3), therefore NAF_1 is used in $R_{\mathrm{MC},1}$. The FRFs of NAF_1, NAF_2 and also an ideal integrator are shown in Fig. 5. The NAF-functions operate as an integrator at specific frequencies $\omega_{\mathrm{C},1}/(2\pi)$ and $\omega_{\mathrm{C},2}/(2\pi)$. For the implementation on the control logic, the transfer functions are discretised with the bilinear transform.

At this point it is necessary to find the gain values of the controllers. To do this, each of the four controllers is investigated individually for different gains and the others are set to zero. Like before, the systems FRFs are measured and $G_{22}(\mathrm{j}\omega)$ from actuator two $f_{\mathrm{A},2}$ to sensor two $q_{\mathrm{S},2}$ is displayed in Fig. 6 for each measurement.

Both of the local controllers act on mode one and two. $R_{\mathrm{LC},1}$ achieves a good damping rate at 83.5 Hz, which is the second mode (see Fig. 6, top left). The first one is also slightly damped for small gains. However, when $k_{\mathrm{LC},1}$ is increased, the amplitude of $G_{22}(\mathrm{j}\omega)$ rises. So the best value is found to be $k_{\mathrm{LC},1} = 1000$. The behaviour of the second local controller

$R_{\mathrm{LC},2}$ is quiet similar (see Fig. 6, bottom left), but it shows a better performance on mode one and the damping of the second peak is limited. Therefore, the second controller gain is set to be $k_{\mathrm{LC},2} = 2000$.

By looking at the right side of Fig. 6, it can be seen that each modal controller is acting on only one of the systems modes and does not affect the other. Furthermore, $R_{\mathrm{MC},2}$ is the only controller that has a negligible effect on the peak at approx. 280 Hz. This is because this vibration mode has a very small amplitude in the FRF $G_{\mathrm{mod},22}(\mathrm{j}\omega)$ in Fig. 3.

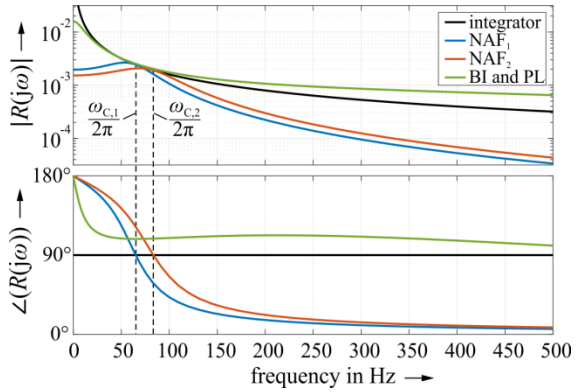

Fig. 5. FRFs of the implemented controllers

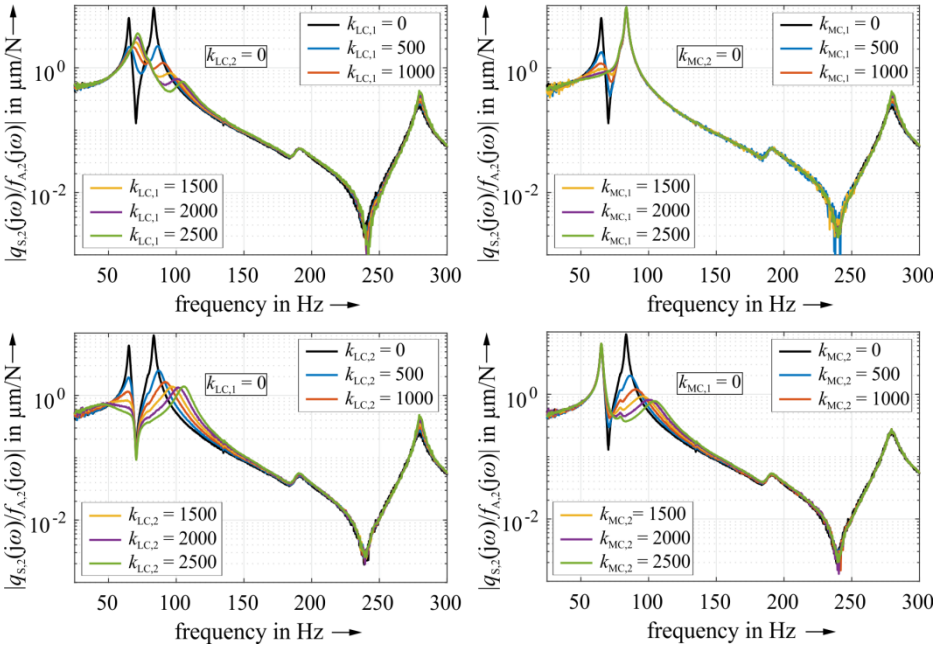

Fig. 6. Measured FRF with different controller gains (excitation with ADD): LC 1 (top, left), LC 2 (bottom, left), MC 1 (top, right) and MC 2 (bottom, right)

After tuning each controller separately, both controllers of LC and MC are activated simultaneously and the gains that achieved the best results in Fig. 6, are used. For this investigation, the FRFs from f_{Imp} to q_{Imp} are measured because this shows the systems reaction to disturbances (see Fig. 7). The yellow line, that still shows a peak at about 105 Hz,

displays the response with the gains that have been mentioned previously. However, the behaviour of the system can be improved by tuning the gains in another way (purple line). The MC provides good results (red line) when the gains of the independent tuning are used, and no further adaptation is necessary. Looking at the peak at around 280 Hz, the LC causes a higher increase of the amplitude than the MC.

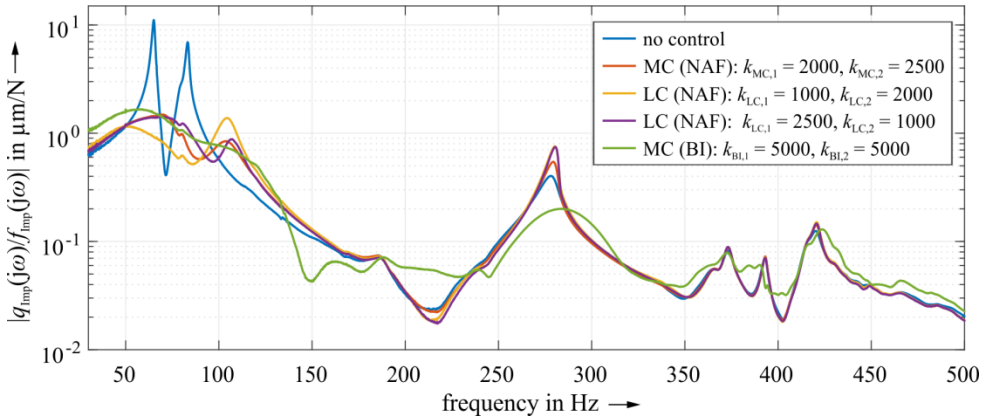

Fig. 7. Comparison of measured FRF for different control strategies (excitation with an impulse hammer)

4.3. IMPROVEMENT OF THE CONTROL STRATEGY

Since the NAF control law has to be tuned to the systems eigenfrequencies, it is sensitive to parameter variations. In this section, another control law is investigated, which is able to damp a wider range of frequencies. The new transfer function of the first modal controller is defined by:

$$R_{\mathrm{MC},1} = -\underbrace{k_{\mathrm{BI},1}}_{\text{gain}} \cdot \underbrace{\underbrace{\frac{1}{\mathrm{j}\omega}}_{\mathrm{I}} \cdot \underbrace{\frac{\mathrm{j}\omega}{(\mathrm{j}\omega+\omega_{\mathrm{H}})}}_{\mathrm{HP}} \cdot \underbrace{\frac{1}{(\mathrm{j}\omega+\omega_{\mathrm{L}})}}_{\mathrm{LP}}}_{\mathrm{BI}} \cdot \underbrace{\frac{(\mathrm{j}\omega+\omega_1)}{(\mathrm{j}\omega+\omega_2)}}_{\mathrm{PL}} = \frac{-k_{\mathrm{BI},1}(\mathrm{j}\omega+\omega_1)}{(\mathrm{j}\omega+\omega_{\mathrm{H}})(\mathrm{j}\omega+\omega_L)(\mathrm{j}\omega+\omega_2)}. \tag{21}$$

The main part of Eq. (21) is the integrator (I) in combination with the high-pass (HP), which allows the pole to be removed at $\omega = 0$ Hz [10]. This avoids stability issues at low frequencies. With an additional low-pass, this function is called a *band-limited integrator* (BI) in this paper. The last part of Eq. (21) is a phase-lead compensator (PL), that in this case, improves the behaviour of the controller at the 280 Hz peak. The control law of the second modal controller is equal to the first one, but without the PL compensator, because there is no influence on the peaks between 200 Hz and 500 Hz since they do not appear in $G_{\mathrm{mod},22}$ (compare Fig. 3). The FRF of Eq. (21) is illustrated in Fig. 5 as green curve.

The result is shown in Fig. 7 (green line), where $\omega_{\mathrm{H}} = 20\pi$ rad/s, $\omega_{\mathrm{L}} = 2000\pi$ rad/s, $\omega_1 = 400\pi$ rad/s and $\omega_2 = 1600\pi$ rad/s are used. As with the NAF used before, this approach achieves a good damping effect at the first and second normal mode. Furthermore, the amplitude at about 280 Hz is reduced. Disadvantageously, there is an increase in the amplitude at low frequencies around 50 Hz, which is caused by the high amplification

of $R_{\mathrm{MC},1}$ in this range (see green line in Fig. 5). Moreover, the mechanical transmission behaviour of the actuator, specified in Eq. (14), is not ideal at low frequencies.

5. CONCLUSION AND OUTLOOK

In this paper, an investigation on the modal vibration control with inertial actuators on the example of an elastic system is presented. The modal control is compared with a local control approach. Both approaches achieved good damping results, when the NAF control law is used. The advantage of the modal control is that the parameter tuning is much easier than with the local method because, when the system is decoupled, the single control loops can be adjusted independently and do not disturb each other. Finally, a modal control applying a band-limited integrator as control law is designed, whereby the knowledge of the exact eigenfrequencies of the system is unnecessary. Therefore, it is insensitive to parameter variations.

In the future, the structure examined in this paper will be extended to a moving bridge of a gantry feed drive. For this purpose, two linear direct drives will be used. The aim is to design a four-variable modal control to achieve vibration as well as position control, where the rigid-body modes of the system are taken into account. Since every actuator and sensor is used in each control task, precise motion and high dynamic stiffness is expected. Further research will be carried out to investigate the modal control when the dynamic behaviour of the system changes e.g. as a function of the moving masses.

ACKNOWLEDGMENTS

This research was supported by a German Research Foundation (DFG) grant, received within the research project 'Fundamental analysis of the modal control applied to over-actuated machine tools' (IH 124/4-1), which is gratefully acknowledged. We would like to thank the Fraunhofer IWU – Machine Tool Department, in particular Dr. Bergmann and Mr. Wabner for providing technical equipment.

REFERENCES

[1] PEUKERT C., MERX M., MÜLLER J., IHLENFELDT S., 2017, *Flexible coupling of drive and guide elements for parallel-driven feed axes to increase dynamics and accuracy of motion*, Journal of Machine Engineering, 17/2, 77–89.

[2] MERX M., PEUKERT C., MÜLLER J., IHLENFELDT S., 2017, *Kinematically Coupled Force-Compensation – experimental and simulative investigation with a highly dynamic test bed*, In: SCHMIDT R. (ed.), SCHUH G. (ed.), 7th WGP-Jahreskongress 2017, Aachen, 383–390.

[3] IHLENFELDT S., MÜLLER J., MERX M., PEUKERT C., 2018, *A Novel concept for highly dynamic over-actuated lightweight machine tools*, In: YAN X. (ed.), BRADLEY D. (ed.), MOORE P. (ed.), Reinventing Mechatronics, Proceedings of Mechatronics, Glasgow, 210–216.

[4] KROLL L., BLAU P., WABNER M., FRIEß U., EULITZ J., KLÄRNER M., 2011, *Lightweight components for energy-efficient machine tools*, CIRP Journal of Manufacturing Science and Technology, 4/2, 148–160.

[5] MÖHRING H.-C., BRECHER C., ABELE E., FLEISCHER J., BLEICHER F., 2015, *Materials in machine tool structures*, CIRP Annals – Manufacturing Technology, 64/2, 725–748.

[6] HESSELBACH J., 2011, *Adaptronik für Werkzeugmaschinen: Forschung in Deutschland* (*Berichte aus dem Maschinenbau*).
[7] ALTINTAS Y., WECK M., 2004, *Chatter stability of metal cutting and grinding*, CIRP Annals – Manufacturing Technology, 53/2, 619–642.
[8] LÖSER M., OTTO A., IHLENFELDT S., RADONS G., 2018, *Chatter prediction for uncertain parameters*, Advances in Manufacturing, 6/3, 310–333.
[9] BRECHER C., BAUMLER S., BROCKMANN B., 2013, *Avoiding chatter by means of active damping systems for machine tools*, Journal of Machine Engineering, 13/3, 117–128.
[10] LAW M., WABNER M., FRIESS U., IHLENFELDT S., 2014, *Improving machining performance of in-use machine tools with active damping devices*, 3rd International Chemnitz Manufacturing Colloquium ICMC 2014, Chemnitz, 393–412..
[11] LOPEZ DE LACALLE N., LAMIKIZ A., 2009, *Machine Tools for Removal Processes: A General View*, Machine Tools for High Performance Machining, 1–45.
[12] SIMNOFSKE M., HESSELBACH J., 2006, *The increase of the dynamic and static stiffness of a grinding machine*, ASME, 30th Annual Mechanisms and Robotics Conference, Philadelphia, 2, 23–30.
[13] DENKENA B., GÜMMER O., 2012, *Process stabilization with an adaptronic spindle system*, Production Engineering, 6/4-5, 485–492.
[14] KRAS A., BOURGAIN F., CLAEYSSEN F., 2014, *Amplified piezo actuator APA® with viscoelastic material for machine tool semi-active damping system*, Journal of Machine Engineering, 14/3, 83–96.
[15] SINGER N.C., SEERING W.P., 1990, *Preshaping command inputs to reduce system vibration*, Journal of Dynamic Systems, Measurement, and Control, 112/1, 76–82.
[16] PEREIRA E., TRAPERO J.R., DÍAZ I.M., FELIU V, 2012, *Adaptive input shaping for single-link flexible manipulators using an algebraic identification,* Control Engineering Practice, 20/2, 138–147.
[17] ZHANG Q., LI C., ZHANG J., JIN J., 2016, Active vibration control and coupled vibration analysis of a parallel manipulator with multiple flexible links, Shock and Vibration, Article number 7474085.
[18] MEIROVITCH L., BARUH H., ÖZ H., 1983, *A Comparison of control techniques for large flexible systems*, Journal of Guidance, Control, and Dynamics, 6/4, 302–310.
[19] BALAS M.J., 1978, *Active control of flexible systems*, Journal of Optimization Theory and Applications, 25/3, 415–436.
[20] MEIROVITCH L., BARUH H., 1983, *On the problem of observation spillover in self-adjoint distributed-parameter systems*, Journal of Optimization Theory and Applications, 39/2, 269–291.
[21] INMAN D. J., 2001, *Active modal control for smart structures*, Philosophical Transactions of the Royal Society, 359, 205–219.
[22] SKIDMORE G.R., HALLAUER JR.W.L., 1985, *Modal-Space active damping of a beam-cable structure: theory and experiment*, Journal of Sound and Vibration, 101/2, 149–160.
[23] KHULIEF Y.A., 2001, *Active modal control of vibrations in elastic structures in the presence of material damping*, Computer Methods in Applied Mechanics and Engineering, 190/51–52, 6947–6961.
[24] LINDBERG R.E., LONGMAN R.W., 1984, *On the number and placement of actuators for independent modal space control*, Journal of Guidance, Control, and Dynamics, 7/2, 215–221.
[25] BAZ A., POH S., 1990, *Experimental implementation of the modified independent modal space control method*, Journal of Sound and Vibration, 139/1, 133–149.
[26] BELYAEV A.K., FEDOTOV A.V., IRSCHIK H., NADER M., POLYANSKIY V.A., SMIRNOVA N.A., 2017, *Experimental study of local and modal approaches to active vibration control of elastic systems*, Structure Control & Health Monitoring, 25/2.
[27] RESTA F., RIPAMONTI F., CAZZULANI G., FERRARI M., 2010, *Independent modal control for nonlinear flexible structures: An experimental test rig*, Journal of Sound and Vibration, 329/8, 961–972.
[28] ZHANG Q., JIN J., ZHANG J., ZHAO C., 2014, *Active vibration suppression of a 3-DOF flexible parallel manipulator using Efficient Modal Control*, Shock and Vibration, Article number 953694.
[29] SCHAECHTER D.B., *Optimal local Control of Flexible Structures*, 1981, Journal of Guidance, Control, and Dynamics, 4/1, 22–26.
[30] GINSBERG J.H., 2001, *Mechanical and structural vibrations: theory and applications*, Wiley, 704.
[31] MEIROVITCH L., BARUH H., 1985, *The implementation of modal filters for control of structures*, Journal of Guidance, Control, and Dynamics, 8/6, 707–716.
[32] BRAGHIN F., CINQUEMANI S., RESTA F., 2012, *A new approach to the synthesis of modal control laws in active structural vibration control*, Journal of Vibration and Control, 19/2, 163–182.
[33] CAZZULANI G., RESTA F., RIPAMONTI F., ZANZI R., 2012, Negative derivative feedback for vibration control of flexible structures, Smart Materials and Structures, 21, 075024.

[34] PREUMONT A., 2011, Vibration control of active structures: an introduction, Solid Mechanics and Its Applications, DOI: 10.1007/978-94-007-2033-6.
[35] FANSON J. L., CAUGHEY T. K., 1990, *Positive position feedback control for large space structures*, AIAA Journal, 28/4, 717–724.
[36] GOH C.J., CAUGHEY T.K., 1985, *On the stability problem caused by finite actuator dynamics in the collocated control of large space structures*, International Journal of Control, 41/3; 787–802.
[37] KIM S.-M., WANG S., BRENNAN M.J., 2011, *Comparison of negative and positive position feedback control of a flexible structure*, Smart Materials and Structures, 20, 015011.